ARTICLES

Anthropogenic ocean acidification over the twenty-first century and its impact on calcifying organisms

James C. Orr[1], Victoria J. Fabry[2], Olivier Aumont[3], Laurent Bopp[1], Scott C. Doney[4], Richard A. Feely[5], Anand Gnanadesikan[6], Nicolas Gruber[7], Akio Ishida[8], Fortunat Joos[9], Robert M. Key[10], Keith Lindsay[11], Ernst Maier-Reimer[12], Richard Matear[13], Patrick Monfray[1]†, Anne Mouchet[14], Raymond G. Najjar[15], Gian-Kasper Plattner[7,9], Keith B. Rodgers[1,16]†, Christopher L. Sabine[5], Jorge L. Sarmiento[10], Reiner Schlitzer[17], Richard D. Slater[10], Ian J. Totterdell[18]†, Marie-France Weirig[17], Yasuhiro Yamanaka[8] & Andrew Yool[18]

Today's surface ocean is saturated with respect to calcium carbonate, but increasing atmospheric carbon dioxide concentrations are reducing ocean pH and carbonate ion concentrations, and thus the level of calcium carbonate saturation. Experimental evidence suggests that if these trends continue, key marine organisms—such as corals and some plankton—will have difficulty maintaining their external calcium carbonate skeletons. Here we use 13 models of the ocean–carbon cycle to assess calcium carbonate saturation under the IS92a 'business-as-usual' scenario for future emissions of anthropogenic carbon dioxide. In our projections, Southern Ocean surface waters will begin to become undersaturated with respect to aragonite, a metastable form of calcium carbonate, by the year 2050. By 2100, this undersaturation could extend throughout the entire Southern Ocean and into the subarctic Pacific Ocean. When live pteropods were exposed to our predicted level of undersaturation during a two-day shipboard experiment, their aragonite shells showed notable dissolution. Our findings indicate that conditions detrimental to high-latitude ecosystems could develop within decades, not centuries as suggested previously.

Ocean uptake of CO_2 will help moderate future climate change, but the associated chemistry, namely hydrolysis of CO_2 in seawater, increases the hydrogen ion concentration $[H^+]$. Surface ocean pH is already 0.1 unit lower than preindustrial values. By the end of the century, it will become another 0.3–0.4 units lower[1,2] under the IS92a scenario, which translates to a 100–150% increase in $[H^+]$. Simultaneously, aqueous CO_2 concentrations $[CO_2(aq)]$ will increase and carbonate ion concentrations $[CO_3^{2-}]$ will decrease, making it more difficult for marine calcifying organisms to form biogenic calcium carbonate ($CaCO_3$). Substantial experimental evidence indicates that calcification rates will decrease in low-latitude corals[3–5], which form reefs out of aragonite, and in phytoplankton that form their tests (shells) out of calcite[6,7], the stable form of $CaCO_3$. Calcification rates will decline along with $[CO_3^{2-}]$ owing to its reaction with increasing concentrations of anthropogenic CO_2 according to the following reaction:

$$CO_2 + CO_3^{2-} + H_2O \rightarrow 2HCO_3^- \quad (1)$$

These rates decline even when surface waters remain supersaturated with respect to $CaCO_3$, a condition that previous studies have predicted will persist for hundreds of years[4,8,9].

Recent predictions of future changes in surface ocean pH and carbonate chemistry have primarily focused on global average conditions[1,2,10] or on low latitude regions[4], where reef-building corals are abundant. Here we focus on future surface and subsurface changes in high latitude regions where planktonic shelled pteropods are prominent components of the upper-ocean biota in the Southern Ocean, Arctic Ocean and subarctic Pacific Ocean[11–15]. Recently, it has been suggested that the cold surface waters in such regions will begin to become undersaturated with respect to aragonite only when atmospheric CO_2 reaches 1,200 p.p.m.v., more than four times the preindustrial level ($4 \times CO_2$) of 280 p.p.m.v. (ref. 9). In contrast, our results suggest that some polar and subpolar surface waters will become undersaturated at $\sim 2 \times CO_2$, probably within the next 50 years.

[1]Laboratoire des Sciences du Climat et de l'Environnement, UMR CEA-CNRS, CEA Saclay, F-91191 Gif-sur-Yvette, France. [2]Department of Biological Sciences, California State University San Marcos, San Marcos, California 92096-0001, USA. [3]Laboratoire d'Océanographie et du Climat: Expérimentations et Approches Numériques (LOCEAN), Centre IRD de Bretagne, F-29280 Plouzané, France. [4]Woods Hole Oceanographic Institution, Woods Hole, Massachusetts 02543-1543, USA. [5]National Oceanic and Atmospheric Administration (NOAA)/Pacific Marine Environmental Laboratory, Seattle, Washington 98115-6349, USA. [6]NOAA/Geophysical Fluid Dynamics Laboratory, Princeton, New Jersey 08542, USA. [7]Institute of Geophysics and Planetary Physics, UCLA, Los Angeles, California 90095-4996, USA. [8]Frontier Research Center for Global Change, Yokohama 236-0001, Japan. [9]Climate and Environmental Physics, Physics Institute, University of Bern, CH-3012 Bern, Switzerland. [10]Atmospheric and Oceanic Sciences (AOS) Program, Princeton University, Princeton, New Jersey 08544-0710, USA. [11]National Center for Atmospheric Research, Boulder, Colorado 80307-3000, USA. [12]Max Planck Institut für Meteorologie, D-20146 Hamburg, Germany. [13]CSIRO Marine Research and Antarctic Climate and Ecosystems CRC, Hobart, Tasmania 7001, Australia. [14]Astrophysics and Geophysics Institute, University of Liege, B-4000 Liege, Belgium. [15]Department of Meteorology, Pennsylvania State University, University Park, Pennsylvania 16802-5013, USA. [16]LOCEAN, Université Pierre et Marie Curie, F-75252 Paris, France. [17]Alfred Wegener Institute for Polar and Marine Research, D-27515 Bremerhaven, Germany. [18]National Oceanography Centre Southampton, Southampton SO14 3ZH, UK. †Present addresses: Laboratoire d'Etudes en Géophysique et Océanographie Spatiales, UMR 5566 CNES-CNRS-IRD-UPS, F-31401 Toulouse, France (P.M.); AOS Program, Princeton University, Princeton, New Jersey 08544-0710, USA (K.B.R.); The Met Office, Hadley Centre, FitzRoy Road, Exeter EX1 3PB, UK (I.J.T.).

Changes in carbonate

We have computed modern-day ocean carbonate chemistry from observed alkalinity and dissolved inorganic carbon (DIC), relying on data collected during the CO_2 Survey of the World Ocean Circulation Experiment (WOCE) and the Joint Global Ocean Flux Study (JGOFS). These observations are centred around the year 1994, and have recently been provided as a global-scale, gridded data product GLODAP (ref. 16; see Supplementary Information). Modern-day surface $[CO_3^{2-}]$ varies meridionally by more than a factor of two, from average concentrations in the Southern Ocean of 105 μmol kg^{-1} to average concentrations in tropical waters of 240 μmol kg^{-1} (Fig. 1). Low $[CO_3^{2-}]$ in the Southern Ocean is due to (1) low surface temperatures and CO_2-system thermodynamics, and (2) large amounts of upwelled deep water, which contain high $[CO_2(aq)]$ from organic matter remineralization. These two effects reinforce one another, yielding a high positive correlation of present-day $[CO_3^{2-}]$ with temperature (for example, $R^2 = 0.92$ for annual mean surface maps). Changes in $[CO_3^{2-}]$ and $[CO_2(aq)]$ are also inextricably linked to changes in other carbonate chemistry variables (Supplementary Fig. S1).

We also estimated preindustrial $[CO_3^{2-}]$ from the same data, after subtracting data-based estimates of anthropogenic DIC (ref. 17) from the modern DIC observations and assuming that preindustrial and modern alkalinity fields were identical (see Supplementary Information). Relative to preindustrial conditions, invasion of anthropogenic CO_2 has already reduced modern surface $[CO_3^{2-}]$ by more than 10%, that is, a reduction of 29 μmol kg^{-1} in the tropics and 18 μmol kg^{-1} in the Southern Ocean. Nearly identical results were found when, instead of the data-based anthropogenic CO_2 estimates, we used simulated anthropogenic CO_2, namely the median from 13 models that participated in the second phase of the Ocean Carbon-Cycle Model Intercomparison Project, or OCMIP-2 (Fig. 1c).

To quantify future changes in carbonate chemistry, we used simulated DIC from ocean models that were forced by two atmospheric CO_2 scenarios: the Intergovernmental Panel on Climate Change (IPCC) IS92a 'continually increasing' scenario (788 p.p.m.v. in the year 2100) and the IPCC S650 'stabilization' scenario (563 p.p.m.v. in the year 2100) (Fig. 1). Simulated perturbations in DIC relative to 1994 (the GLODAP reference year) were added to the modern DIC data; again, alkalinity was assumed to be constant. To provide a measure of uncertainty, we report model results as the OCMIP median $\pm 2\sigma$. The median generally outperformed

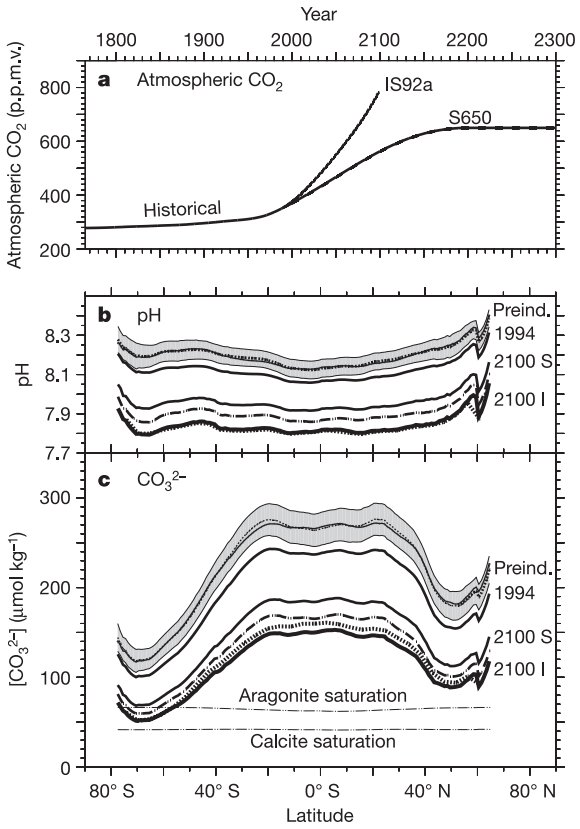

Figure 1 | Increasing atmospheric CO_2 and decreasing surface ocean pH and $[CO_3^{2-}]$. **a**, Atmospheric CO_2 used to force 13 OCMIP models over the industrial period ('Historical') and for two future scenarios: IS92a ('I' in **b** and **c**) and S650 ('S' in **b** and **c**). **b**, **c**, Increases in atmospheric CO_2 lead to reductions in surface ocean pH (**b**) and surface ocean $[CO_3^{2-}]$ (**c**). Results are given as global zonal averages for the 1994 data and the preindustrial ('Preind.') ocean. The latter were obtained by subtracting data-based anthropogenic DIC (ref. 17) (solid line in grey-shaded area), as well as by subtracting model-based anthropogenic DIC (OCMIP median, dotted line in grey-shaded area; OCMIP range, grey shading). Future results for the year 2100 come from the 1994 data plus the simulated DIC perturbations for the two scenarios; results are also shown for the year 2300 with S650 (thick dashed line). The small effect of future climate change simulated by the IPSL climate–carbon model is added as a perturbation to IS92a in the year 2100 (thick dotted line); two other climate–carbon models, PIUB-Bern and Commonwealth Scientific and Industrial Research Organisation (CSIRO), show similar results (Fig. 3a). The thin dashed lines indicating the $[CO_3^{2-}]$ for sea water in equilibrium with aragonite and calcite are nearly flat, revealing weak temperature sensitivity.

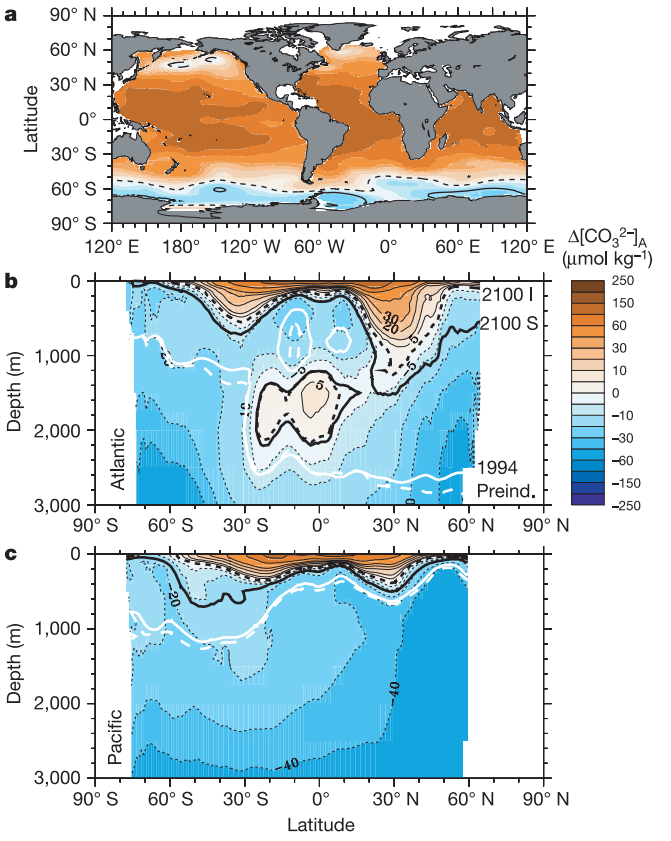

Figure 2 | The aragonite saturation state in the year 2100 as indicated by $\Delta[CO_3^{2-}]_A$. The $\Delta[CO_3^{2-}]_A$ is the *in situ* $[CO_3^{2-}]$ minus that for aragonite-equilibrated sea water at the same salinity, temperature and pressure. Shown are the OCMIP-2 median concentrations in the year 2100 under scenario IS92a: **a**, surface map; **b**, Atlantic; and **c**, Pacific zonal averages. Thick lines indicate the aragonite saturation horizon in 1765 (Preind.; white dashed line), 1994 (white solid line) and 2100 (black solid line for S650; black dashed line for IS92a). Positive $\Delta[CO_3^{2-}]_A$ indicates supersaturation; negative $\Delta[CO_3^{2-}]_A$ indicates undersaturation.

individual models in OCMIP model–data comparison (Supplementary Fig. S2). By the year 2100, as atmospheric CO_2 reaches 788 p.p.m.v. under the IS92a scenario, average tropical surface $[CO_3^{2-}]$ declines to $149 \pm 14\,\mu mol\,kg^{-1}$. This is a 45% reduction relative to preindustrial levels, in agreement with previous predictions[4,8]. In the Southern Ocean (all waters south of 60° S), surface concentrations dip to $55 \pm 5\,\mu mol\,kg^{-1}$, which is 18% below the threshold where aragonite becomes undersaturated ($66\,\mu mol\,kg^{-1}$).

These changes extend well below the sea surface. Throughout the Southern Ocean, the entire water column becomes undersaturated with respect to aragonite. During the twenty-first century, under the IS92a scenario, the Southern Ocean's aragonite saturation horizon (the limit between undersaturation and supersaturation) shoals from its present average depth of 730 m (Supplementary Fig. S3) all the way to the surface (Fig. 2). Simultaneously, in a portion of the subarctic Pacific, the aragonite saturation horizon shoals from depths of about 120 m to the surface. In the North Atlantic, surface waters remain saturated with respect to aragonite, but the aragonite saturation horizon shoals dramatically; for example, north of 50° N it shoals from 2,600 m to 115 m. The greater erosion in the North Atlantic is due to deeper penetration and higher concentrations of anthropogenic CO_2, a tendency that is already evident in present-day data-based estimates[17,18] and in models[19,20] (Supplementary Figs S4 and S5). Less pronounced changes were found for the calcite saturation horizon. For example, in the year 2100 the average calcite saturation horizon in the Southern Ocean stays below 2,200 m. Nonetheless, in 2100 surface waters of the Weddell Sea become slightly undersaturated with respect to calcite.

In the more conservative S650 scenario, the atmosphere reaches $2 \times CO_2$ in the year 2100, 50 years later than with the IS92a scenario. In 2100, Southern Ocean surface waters generally remain slightly supersaturated with respect to aragonite. However, the models also simulate that the Southern Ocean's average aragonite saturation horizon will have shoaled from 730 m to 60 m, and that the entire water column in the Weddell Sea will have become undersaturated (Fig. 2). In the north, all surface waters remain saturated under the S650 scenario. North of 50° N, the annual average aragonite saturation horizon shoals from 140 m to 70 m in the Pacific, whereas it shoals by 2,000 m to 610 m in the North Atlantic. Therefore, under either scenario the OCMIP models simulated large changes in surface and subsurface $[CO_3^{2-}]$. Yet these models account for only the direct geochemical effect of increasing atmospheric CO_2 because they were all forced with prescribed modern-day climate conditions.

In addition to this direct geochemical effect, ocean $[CO_3^{2-}]$ is also altered by climate variability and climate change. To quantify the added effect of future climate change, we analysed results from three atmosphere–ocean climate models that each included an ocean carbon-cycle component (see Supplementary Information). These three models agree that twenty-first century climate change will cause a general increase in surface ocean $[CO_3^{2-}]$ (Fig. 3), mainly because most surface waters will be warmer. However, the models also agree that the magnitude of this increase in $[CO_3^{2-}]$ is small, typically counteracting less than 10% of the decrease due to the geochemical effect. High-latitude surface waters show the smallest increases in $[CO_3^{2-}]$, and even small reductions in some cases. Therefore, our analysis suggests that physical climate change alone will not substantially alter high-latitude surface $[CO_3^{2-}]$ during the twenty-first century.

Climate also varies seasonally and interannually, whereas our previous focus has been on annual changes. To illustrate how climate variability affects surface $[CO_3^{2-}]$, we used results from an ocean carbon-cycle model forced with the daily National Centers for Environmental Prediction (NCEP) reanalysis fields[21] over 1948–2003 (see Supplementary Information). These fields are observationally based and vary on seasonal and interannual timescales. Simulated interannual variability in surface ocean $[CO_3^{2-}]$ is negligible when compared with the magnitude of the anthropogenic decline (Fig. 3b). Seasonal variability is also negligible except in the high latitudes, where surface $[CO_3^{2-}]$ varies by about $\pm 15\,\mu mol\,kg^{-1}$

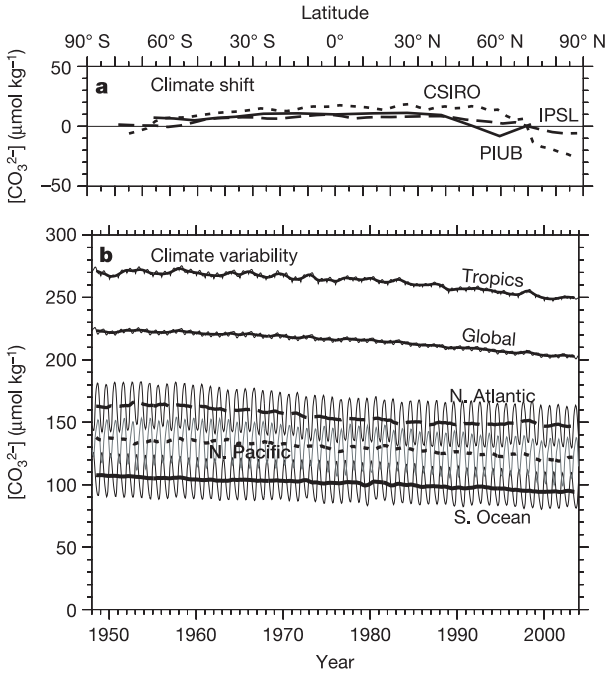

Figure 3 | Climate-induced changes in surface $[CO_3^{2-}]$. **a**, The twenty-first century shift in zonal mean surface ocean $[CO_3^{2-}]$ due to climate change alone, from three atmosphere–ocean climate models—CSIRO-Hobart (short dashed line), IPSL-Paris (long dashed line) and PIUB-Bern (solid line)—that each include an ocean carbon-cycle component (see Supplementary Information). **b**, The regional-scale seasonal and interannual variability is simulated by an ocean carbon-cycle model forced with reanalysed climate forcing.

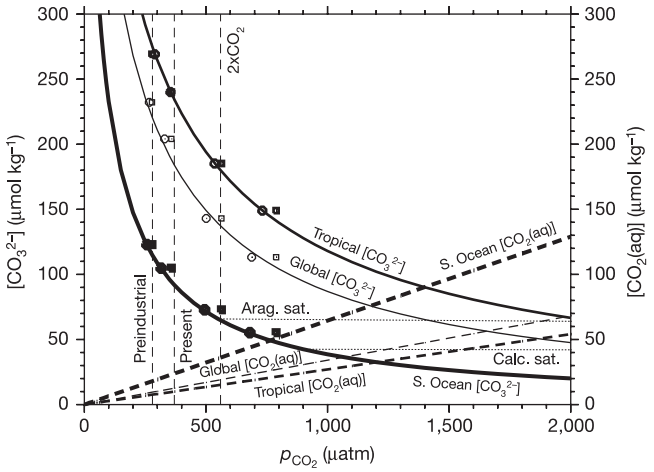

Figure 4 | Key surface carbonate chemistry variables as a function of p_{CO_2}. Shown are both $[CO_3^{2-}]$ (solid lines) and $[CO_2(aq)]$ (dashed lines) for average surface waters in the tropical ocean (thick lines), the Southern Ocean (thickest lines) and the global ocean (thin lines). Solid and dashed lines are calculated from the thermodynamic equilibrium approach. For comparison, open symbols are for $[CO_3^{2-}]$ from our non-equilibrium, model-data approach versus seawater p_{CO_2} (open circles) and atmospheric p_{CO_2} (open squares); symbol thickness corresponds with line thickness, which indicates the regions for area-weighted averages. The nearly flat, thin dotted lines indicate the $[CO_3^{2-}]$ for seawater in equilibrium with aragonite ('Arag. sat.') and calcite ('Calc. sat.').

when averaged over large regions. This is smaller than the twenty-first-century's transient change (for example, ~50 μmol kg^{-1} in the Southern Ocean). However, high-latitude surface waters do become substantially less saturated during winter, because of cooling (resulting in higher [CO_2(aq)]) and greater upwelling of DIC-enriched deep water, in agreement with previous observations in the North Pacific[22]. Thus, high-latitude undersaturation will be first reached during winter.

Our predicted changes may be compared to those found in earlier studies, which focused on surface waters in the tropics[8] and in the subarctic Pacific[22,23]. These studies assumed thermodynamic equilibrium between CO_2 in the atmosphere and the surface waters at their *in situ* alkalinity, temperature and salinity. If, in the equilibrium approach, the p_{CO_2} is taken only to represent seawater p_{CO_2}, then the results agree with our non-equilibrium approach when the sets of carbonate chemistry constants are identical (Fig. 4). However, assuming equilibrium with the atmosphere leads to the prediction that future undersaturation will occur too soon (at lower atmospheric CO_2 levels), mainly because the anthropogenic transient in the ocean actually lags that in the atmosphere. For example, with the equilibrium approach, we predict that average surface waters in the Southern Ocean become undersaturated when atmospheric CO_2 is 550 p.p.m.v. (in the year 2050 under IS92a), whereas our non-equilibrium approach, which uses models and data, indicates that undersaturation will occur at 635 p.p.m.v. (in the year 2070). Despite these differences, both approaches indicate that the Southern Ocean surface waters will probably become undersaturated with respect to aragonite during this century. Conversely, both of these approaches disagree with a recent assessment[9] that used a variant of the standard thermodynamic equilibrium approach, where an incorrect input temperature was used inadvertently.

Uncertainties

The three coupled climate–carbon models show little effect of climate change on surface [CO_3^{2-}] (compare Fig. 3a to Fig. 1) partly because air–sea CO_2 exchange mostly compensates for the changes in surface DIC caused by changes in marine productivity and circulation. In subsurface waters where such compensation is lacking, these models could under- or over-predict how much [CO_3^{2-}] will change as a result of changes in overlying marine productivity. However, the models project a consistent trend, which only worsens the decline in subsurface [CO_3^{2-}]; that is, all coupled climate models predict increased evaporation in the tropics and increased precipitation in the high latitudes[24]. This leads to greater upper ocean stratification in the high latitudes, which in turn decreases nutrients (but not to zero) and increases light availability (owing to more shallow mixed layers). Thus, at 2 × CO_2 there is a 10% local increase in surface-to-deep export of particulate organic carbon (POC) in the Southern Ocean using the Institut Pierre Simon Laplace (IPSL)-Paris model[25]. Subsequent remineralization of this exported POC within the thermocline would increase DIC, which would only exacerbate the decrease in high-latitude subsurface [CO_3^{2-}]. For the twenty-first century, these uncertainties appear small next to the anthropogenic DIC invasion (see Supplementary Information).

The largest uncertainty by far, and the only means to limit the future decline in ocean [CO_3^{2-}], is the atmospheric CO_2 trajectory. To better characterize uncertainty due to CO_2 emissions, we compared the six illustrative IPCC Special Reports on Emission Scenarios (SRES) in the reduced complexity, Physics Institute University of Bern (PIUB)-Bern model. Under the moderate SRES B2 scenario, average Southern Ocean surface waters in that model become undersaturated with respect to aragonite when atmospheric CO_2 reaches 600 p.p.m.v. in the year 2100 (Fig. 5). For the three higher-emission SRES scenarios (A1FI, A2 and A1B), these waters become undersaturated sooner (between the years 2058 and 2073); for the two lower-emission scenarios (A1T and B1), these waters remain slightly supersaturated in 2100. Thus, if atmospheric CO_2 rises above 600 p.p.m.v., most Southern Ocean surface waters will become undersaturated with respect to aragonite. Yet, even below this level, the Southern Ocean's aragonite saturation horizon will shoal substantially (Fig. 2). For a given atmospheric CO_2 scenario, predicted changes in surface ocean [CO_3^{2-}] are much more certain than the related changes in climate. The latter depend not only on the model response to CO_2 forcing, but also on poorly constrained physical processes, such as those associated with clouds.

Ocean CO_2 uptake

With higher levels of anthropogenic CO_2 and lower surface [CO_3^{2-}], the change in surface ocean DIC per unit change in atmospheric CO_2 (μmol kg^{-1} per p.p.m.v.) will be about 60% lower in the year 2100 (under IS92a) than it is today. Simultaneously, the CO_3^{2-}/CO2(aq) ratio will decrease from 4:1 to 1:1 in the Southern Ocean (Fig. 4). These decreases are due to the well-understood anthropogenic reduction in buffer capacity[26], already accounted for in ocean carbon-cycle models.

On the other hand, reduced export of $CaCO_3$ from the high latitudes would increase surface [CO_3^{2-}], thereby increasing ocean CO_2 uptake and decreasing atmospheric CO_2. Owing to this effect, ocean CO_2 uptake could increase by 6–13 petagrams (Pg) C over the twenty-first century, based on one recent model study[27] that incorporated an empirical, CO_2-dependant relationship for calcification[7]. Rates of calcification could decline even further, to zero, if waters actually became undersaturated with respect to both aragonite and calcite. We estimate that the total shutdown of high-latitude aragonite production would lead to, at most, a 0.25 Pg C yr^{-1} increase in ocean CO_2 uptake, assuming that 1 Pg C yr^{-1} of $CaCO_3$ is exported globally[28], that up to half of that is aragonite[9,29], and that perhaps half of all aragonite is exported from the high latitudes. The actual increase in ocean CO_2 uptake could be much lower because the aragonite fraction of the $CaCO_3$ may be only 0.1 based on low-latitude sediment traps[30], and the latitudinal distribution of aragonite export is uncertain. Thus, increased CO_2 uptake from reduced export of aragonite will provide little compensation for decreases in ocean CO_2 uptake due to reductions in buffer capacity. Of greater concern are potential biological impacts due to future undersaturation.

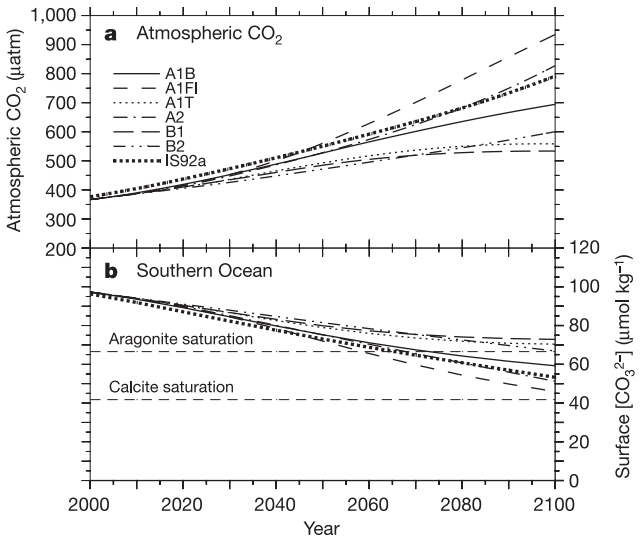

Figure 5 | Average surface [CO_3^{2-}] in the Southern Ocean under various scenarios. Time series of average surface [CO_3^{2-}] in the Southern Ocean for the PIUB-Bern reduced complexity model (see Fig. 3 and Supplementary Information) under the six illustrative IPCC SRES scenarios. The results for the SRES scenarios A1T and A2 are similar to those for the non-SRES scenarios S650 and IS92a, respectively.

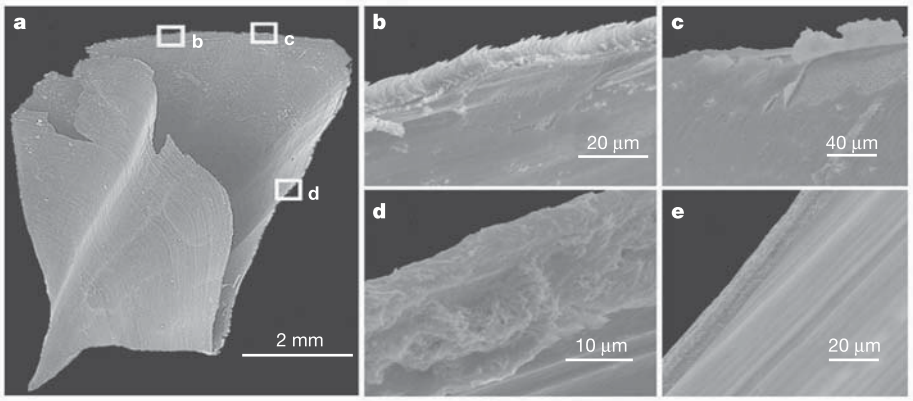

Figure 6 | Shell dissolution in a live pteropod. a–d, Shell from a live pteropod, *Clio pyramidata*, collected from the subarctic Pacific and kept in water undersaturated with respect to aragonite for 48 h. The whole shell (**a**) has superimposed white rectangles that indicate three magnified areas: the shell surface (**b**), which reveals etch pits from dissolution and resulting exposure of aragonitic rods; the prismatic layer (**c**), which has begun to peel back, increasing the surface area over which dissolution occurs; and the aperture region (**d**), which reveals advanced shell dissolution when compared to a typical *C. pyramidata* shell not exposed to undersaturated conditions (**e**).

Biological impacts

The changes in seawater chemistry that we project to occur during this century could have severe consequences for calcifying organisms, particularly shelled pteropods: the major planktonic producers of aragonite. Pteropod population densities are high in polar and subpolar waters. Yet only five species typically occur in such cold water regions and, of these, only one or two species are common at the highest latitudes[31]. High-latitude pteropods have one or two generations per year[12,15,32], form integral components of food webs, and are typically found in the upper 300 m where they may reach densities of hundreds to thousands of individuals per m^3 (refs 11, 13–15). In the Ross Sea, for example, the prominent subpolar–polar pteropod *Limacina helicina* sometimes replaces krill as the dominant zooplankton, and is considered an overall indicator of ecosystem health[33]. In the strongly seasonal high latitudes, sedimentation pulses of pteropods frequently occur just after summer[15,34]. In the Ross Sea, pteropods account for the majority of the annual export flux of both carbonate and organic carbon[34,35]. South of the Antarctic Polar Front, pteropods also dominate the export flux of $CaCO_3$ (ref. 36).

Pteropods may be unable to maintain shells in waters that are undersaturated with respect to aragonite. Data from sediment traps indicate that empty pteropod shells exhibit pitting and partial dissolution as soon as they fall below the aragonite saturation horizon[22,36,37]. *In vitro* measurements confirm such rapid pteropod shell dissolution rates[38]. New experimental evidence suggests that even the shells of live pteropods dissolve rapidly once surface waters become undersaturated with respect to aragonite[9]. Here we show that when the live subarctic pteropod *Clio pyramidata* is subjected to a level of undersaturation similar to what we predict for Southern Ocean surface waters in the year 2100 under IS92a, a marked dissolution occurs at the growing edge of the shell aperture within 48 h (Fig. 6). Etch pits formed on the shell surface at the apertural margin (which is typically ~7-μm-thick) as the <1-μm exterior (prismatic layer) peeled back (Fig. 6c), exposing the underlying aragonitic rods to dissolution. Fourteen individuals were tested. All of them showed similar dissolution along their growing edge, even though they all remained alive. If *C. pyramidata* cannot grow its protective shell, we would not expect it to survive in waters that become undersaturated with respect to aragonite.

If the response of other high-latitude pteropod species to aragonite undersaturation is similar to that of *C. pyramidata*, we hypothesize that these pteropods will not be able to adapt quickly enough to live in the undersaturated conditions that will occur over much of the high-latitude surface ocean during the twenty-first century. Their distributional ranges would then be reduced both within the water column, disrupting vertical migration patterns, and latitudinally, imposing a shift towards lower-latitude surface waters that remain supersaturated with respect to aragonite. At present, we do not know if pteropod species endemic to polar regions could disappear altogether, or if they can make the transition to live in warmer, carbonate-rich waters at lower latitudes under a different ecosystem. If pteropods are excluded from polar and subpolar regions, their predators will be affected immediately. For instance, gymnosomes are zooplankton that feed exclusively on shelled pteropods[33,39]. Pteropods also contribute to the diet of diverse carnivorous zooplankton, myctophid and notothenid fishes[40–42], North Pacific salmon[43,44], mackerel, herring, cod and baleen whales[45].

Surface dwelling calcitic plankton, such as foraminifera and coccolithophorids, may fare better in the short term. However, the beginnings of high-latitude calcite undersaturation will only lag that for aragonite by 50–100 years. The diverse benthic calcareous organisms in high-latitude regions may also be threatened, including cold-water corals which provide essential fish habitat[46]. Cold-water corals seem much less abundant in the North Pacific than in the North Atlantic[46], where the aragonite saturation horizon is much deeper (Fig. 2). Moreover, some important taxa in Arctic and Antarctic benthic communities secrete magnesian calcite, which can be more soluble than aragonite. These include gorgonians[46], coralline red algae and echinoderms (sea urchins)[47]. At $2 \times CO_2$, juvenile echinoderms stopped growing and produced more brittle and fragile exoskeletons in a subtropical six-month manipulative experiment[48]. However, the responses of high-latitude calcifiers to reduced $[CO_3^{2-}]$ have generally not been studied. Yet experimental evidence from many lower-latitude, shallow-dwelling calcifiers reveals a reduced ability to calcify with a decreasing carbonate saturation state[9]. Given that at $2 \times CO_2$, calcification rates in some shallow-dwelling calcareous organisms may decline by up to 50% (ref. 9), some calcifiers could have difficulty surviving long enough even to experience undersaturation. Certainly, they have not experienced undersaturation for at least the last 400,000 years[49], and probably much longer[50].

Changes in high-latitude seawater chemistry that will occur by the end of the century could well alter the structure and biodiversity of polar ecosystems, with impacts on multiple trophic levels. Assessing these impacts is impeded by the scarcity of relevant data.

Received 15 June; accepted 29 July 2005.

1. Haugan, P. M. & Drange, H. Effects of CO_2 on the ocean environment. *Energy Convers. Mgmt* **37**, 1019–1022 (1996).

2. Brewer, P. G. Ocean chemistry of the fossil fuel CO_2 signal: the haline signal of "business as usual". *Geophys. Res. Lett.* **24,** 1367–1369 (1997).
3. Gattuso, J.-P., Frankignoulle, M., Bourge, I., Romaine, S. & Buddemeier, R. W. Effect of calcium carbonate saturation of seawater on coral calcification. *Glob. Planet. Change* **18,** 37–46 (1998).
4. Kleypas, J. A. *et al.* Geochemical consequences of increased atmospheric carbon dioxide on coral reefs. *Science* **284,** 118–120 (1999).
5. Langdon, C. *et al.* Effect of elevated CO_2 on the community metabolism of an experimental coral reef. *Glob. Biogeochem. Cycles* **17,** 1011, doi:10.1029/2002GB001941 (2003).
6. Riebesell, U. *et al.* Reduced calcification of marine plankton in response to increased atmospheric CO_2. *Nature* **407,** 364–367 (2000).
7. Zondervan, I., Zeebe, R., Rost, B. & Riebesell, U. Decreasing marine biogenic calcification: A negative feedback on rising atmospheric p_{CO_2}. *Glob. Biogeochem. Cycles* **15,** 507–516 (2001).
8. Broecker, W. S. & Peng, T.-H. Fate of fossil fuel carbon dioxide and the global carbon budget. *Science* **206,** 409–418 (1979).
9. Feely, R. A. *et al.* The impact of anthropogenic CO_2 on the $CaCO_3$ system in the oceans. *Science* **305,** 362–366 (2004).
10. Caldeira, K. & Wickett, M. E. Anthropogenic carbon and ocean pH. *Nature* **425,** 365 (2003).
11. Urban-Rich, J., Dagg, M. & Peterson, J. Copepod grazing on phytoplankton in the Pacific sector of the Antarctic Polar Front. *Deep-Sea Res. II* **48,** 4223–4246 (2001).
12. Kobayashi, H. A. Growth cycle and related vertical distribution of the thecosomatous pteropod *Spiratella "Limacina" helicina* in the central Arctic Ocean. *Mar. Biol.* **26,** 295–301 (1974).
13. Pakhomov, E. A., Verheye, H. M., Atkinson, A., Laubscher, R. K. & Taunton-Clark, J. Structure and grazing impact of the mesozooplankton community during late summer 1994 near South Georgia, Antarctica. *Polar Biol.* **18,** 180–192 (1997).
14. Fabry, V. J. Aragonite production by pteropod molluscs in the subarctic Pacific. *Deep-Sea Res. I* **36,** 1735–1751 (1989).
15. Bathmann, U., Noji, T. T. & von Bodungen, B. Sedimentation of pteropods in the Norwegian Sea in autumn. *Deep-Sea Res.* **38,** 1341–1360 (1991).
16. Key, R. M. *et al.* A global ocean carbon climatology: Results from Global Data Analysis Project (GLODAP). *Glob. Biogeochem. Cycles* **18,** 4031, doi:10.1029/2004GB002247 (2004).
17. Sabine, C. L. *et al.* The ocean sink for anthropogenic CO_2. *Science* **305,** 367–370 (2004).
18. Gruber, N. Anthropogenic CO_2 in the Atlantic Ocean. *Glob. Biogeochem. Cycles* **12,** 165–191 (1998).
19. Sarmiento, J. L., Orr, J. C. & Siegenthaler, U. A perturbation simulation of CO_2 uptake in an ocean general circulation model. *J. Geophys. Res.* **97,** 3621–3645 (1992).
20. Orr, J. C. *et al.* Estimates of anthropogenic carbon uptake from four three-dimensional global ocean models. *Glob. Biogeochem. Cycles* **15,** 43–60 (2001).
21. Kalnay, E. *et al.* The NCEP/NCAR 40-year reanalysis project. *Bull. Am. Meteorol. Soc.* **77,** 437–471 (1996).
22. Feely, R. A. *et al.* Winter–summer variations of calcite and aragonite saturation in the northeast Pacific. *Mar. Chem.* **25,** 227–241 (1988).
23. Feely, R. A., Byrne, R. H., Betzer, P. R., Gendron, J. F. & Acker, J. G. Factors influencing the degree of saturation of the surface and intermediate waters of the North Pacific Ocean with respect to aragonite. *J. Geophys. Res.* **89,** 10631–10640 (1984).
24. Sarmiento, J. L. *et al.* Response of ocean ecosystems to climate warming. *Glob. Biogeochem. Cycles* **18,** 3003, doi:10.1029/2003GB002134 (2004).
25. Bopp, L. *et al.* Potential impact of climate change of marine export production. *Glob. Biogeochem. Cycles* **15,** 81–99 (2001).
26. Sarmiento, J. L., Le Quéré, C. & Pacala, S. Limiting future atmospheric carbon dioxide. *Glob. Biogeochem. Cycles* **9,** 121–137 (1995).
27. Heinze, C. Simulating oceanic $CaCO_3$ export production in the greenhouse. *Geophys. Res. Lett.* **31,** L16308, doi:10.1029/2004GL020613 (2004).
28. Iglesias-Rodriguez, M. D. *et al.* Representing key phytoplankton functional groups in ocean carbon cycle models: Coccolithophorids. *Glob. Biogeochem. Cycles* **16,** 1100, doi:10.1029/2001GB001454 (2002).
29. Berner, R. A. in *The Fate of Fossil Fuel CO_2 in the Oceans* (eds Andersen, N. R. & Malahoff, A.) 243–260 (Plenum, New York, 1977).
30. Fabry, V. J. Shell growth rates of pteropod and heteropod molluscs and aragonite production in the open ocean: Implications for the marine carbonate system. *J. Mar. Res.* **48,** 209–222 (1990).
31. Bé, A. W. H. & Gilmer, R. W. *Oceanic Micropaleontology* **Vol. 1** (ed. Ramsey, A.) 733–808 (Academic, London, 1977).
32. Dadon, J. R. & de Cidre, L. L. The reproductive cycle of the Thecosomatous pteropod *Limacina retroversa* in the western South Atlantic. *Mar. Biol.* **114,** 439–442 (1992).
33. Seibel, B. A. & Dierssen, H. M. Cascading trophic impacts of reduced biomass in the Ross Sea, Antarctica: Just the tip of the iceberg? *Biol. Bull.* **205,** 93–97 (2003).
34. Accornero, A., Manno, C., Esposito, F. & Gambi, M. C. The vertical flux of particulate matter in the polyna of Terra Nova Bay. Part II. Biological components. *Antarct. Sci.* **15,** 175–188 (2003).
35. Collier, R., Dymond, J., Susumu Honjo, S. M., Francois, R. & Dunbar, R. The vertical flux of biogenic and lithogenic material in the Ross Sea: moored sediment trap observations 1996–1998. *Deep-Sea Res. II* **47,** 3491–3520 (2000).
36. Honjo, S., Francois, R., Manganini, S., Dymond, J. & Collier, R. Particle fluxes to the interior of the Southern Ocean in the western Pacific sector along 170° W. *Deep-Sea Res. II* **47,** 3521–3548 (2000).
37. Betzer, P. R., Byrne, R., Acker, J., Lewis, C. S. & Jolley, R. R. The oceanic carbonate system: a reassessment of biogenic controls. *Science* **226,** 1074–1077 (1984).
38. Byrne, R. H., Acker, J. G., Betzer, P. R., Feely, R. A. & Cates, M. H. Water column dissolution of aragonite in the Pacific Ocean. *Nature* **312,** 321–326 (1984).
39. Lalli, C. M. Structure and function of the buccal apparatus of *Clione limacina* (Phipps) with a review of feeding in gymnosomatous pteropods. *J. Exp. Mar. Biol. Ecol.* **4,** 101–118 (1970).
40. Foster, B. A. & Montgomery, J. C. Planktivory in benthic notothenid fish in McMurdo Sound, Antarctica. *Environ. Biol. Fish.* **36,** 313–318 (1993).
41. Pakhomov, E., Perissinotto, A. & McQuaid, C. D. Prey composition and daily rations of myctophid fishes in the Southern Ocean. *Mar. Ecol. Prog. Ser.* **134,** 1–14 (1996).
42. La Mesa, M., Vacchi, M. & Sertorio, T. Z. Feeding plasticity of *Trematomus newnesi* (Pisces, Nototheniidae) in Terra Nova Bay, Ross Sea, in relation to environmental conditions. *Polar Biol.* **23,** 38–45 (2000).
43. Willette, T. M. *et al.* Ecological processes influencing mortality of juvenile pink salmon (*Oncorhynchus gorbuscha*) in Prince William Sound, Alaska. *Fish. Oceanogr.* **10,** 14–41 (2001).
44. Boldt, J. L. & Haldorson, L. J. Seasonal and geographical variation in juvenile pink salmon diets in the Northern Gulf of Alaska and Prince William Sound. *Trans. Am. Fisheries Soc.* **132,** 1035–1052 (2003).
45. Lalli, C. M. & Gilmer, R. *Pelagic Snails* (Stanford Univ. Press, Stanford, 1989).
46. Freiwald, A., Fosså, J. H., Grehan, A., Koslow, T. & Roberts, J. M. *Cold-water Coral Reefs: Out of Sight—No Longer Out of Mind* (No. 22 in Biodiversity Series, UNEP-WCMC, Cambridge, UK, 2004).
47. Dayton, P. K. in *Polar Oceanography, Part B: Chemistry, Biology and Geology* (ed. Smith, W. O.) 631–685 (Academic, San Diego, 1990).
48. Shirayama, Y. & Thornton, H. Effect of increased atmospheric CO_2 on shallow-water marine benthos. *J. Geophys. Res.* **110,** C09S09, doi:10.1029/2004JC002561 (2005).
49. Petit, J. R. *et al.* Climate and atmospheric history of the past 420,000 years from the Vostok ice core, Antarctica. *Nature* **399,** 429–436 (1999).
50. Pearson, P. N. & Palmer, M. R. Middle Eocene seawater pH and atmospheric carbon dioxide concentrations. *Science* **284,** 1824–1826 (1999).

Supplementary Information is linked to the online version of the paper at www.nature.com/nature.

Acknowledgements We thank M. Gehlen for discussions, and J.-M. Epitalon, P. Brockmann and the Ferret developers for help with analysis. All but the climate simulations were made as part of the OCMIP project, which was launched in 1995 by the Global Analysis, Integration and Modelling (GAIM) Task Force of the International Geosphere–Biosphere Programme (IGBP) with funding from NASA (National Aeronautics and Space Administration). OCMIP-2 was supported by the European Union Global Ocean Storage of Anthropogenic Carbon (EU GOSAC) project and the United States JGOFS Synthesis and Modeling Project funded through NASA. The interannual simulation was supported by the EU Northern Ocean Carbon Exchange Study (NOCES) project, which is part of OCMIP-3.

Author Information Reprints and permissions information is available at npg.nature.com/reprintsandpermissions. The authors declare no competing financial interests. Correspondence and requests for materials should be addressed to J.C.O. (orr@cea.fr).